Extended Abstracts of the 2019 International Conference on Solid State Devices and Materials, Nagoya, 2019, pp17-18

Processing rules and materials in high-resolution printing for electronic devices

Yasuyuki Kusaka[1]

[1] National Institute of Advanced Industrial Science and Technology (AIST)
1-1-1 Higashi, Tsukuba
Ibaraki 305-8565, Japan
Phone: +81-29-860-5707 E-mail: y-kusaka@aist.go.jp

Abstract

Printing is a universal tool for the patterning of wet functional materials. Semidried ink layers that exhibit fragile solid behaviors allow us to generate well-defined patterns while withstanding the structural integrity and reproducibility through the transfer of the layers, thus applications to various devices are expected. Here, the conception for material formulations including nanoparticles and small molecule precursors is introduced together with a detailed patterning mechanism. Processing rules for a better pattern fidelity, vertical interconnection formations and high-speed printing are shown where the deformation of blanket materials plays a key role.

1. Introduction

With the advancement of novel wet nanomaterials, various attempts have been made to apply printing technology to functioning devices and components including thin-film transistors (TFT), resistive memory, color filter, quantum dots, fine-pitch interconnection, biosensors and metamaterials. Depending on device specifications, an adequate printing method is chosen so that desired structures can be generated. Typical candidates include screen printing, inkjet printing, gravure offset printing and reverse offset printing. Among them, gravure offset printing and reverse offset printing use poly(dimethylsiloxane) (PDMS) so that patterns formed on the PDMS can be solidified via the absorption of solvents before the transfer onto substrate. The solidification or semidrying of inks has advantages to avoid spreading and dewetting on the substrate owning to Laplace pressure; thereby much finer resolution can be attained (7~10 μm in gravure offset printing and <1~5 μm in reverse offset printing). Here, we focus on reverse offset printing and discuss the following aspects uniquely appeared in the corresponding method:

(i) the patterning mechanism as not wetting but fracture of ink layers is involved,

(ii) an ink formulation scheme to bestow the semidrying capability,

(iii) roles of contact mechanics and the deformation of PDMS during the patterning in processing rules

2. Reverse offset printing

In reverse offset printing, an ink is first uniformly coated on a PDMS sheet called a blanket. After waiting to attain a semidried state, a cliché (typically glass with a relief structure) is brought into contact to remove unnecessary parts of the ink. Then, the remained part of the layer corresponding to the pattern was transferred onto substrate. A schematic of the process is shown in Fig. 1 together with an example of ROP-patterns.

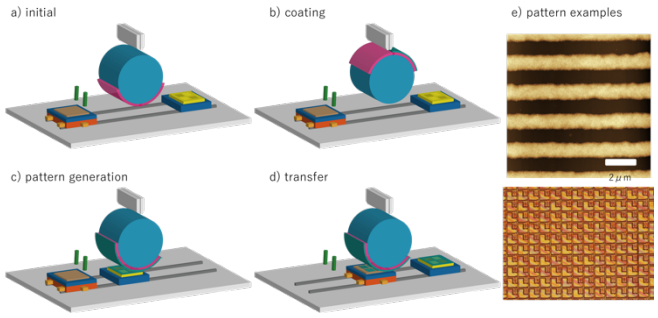

Fig.1 A schematic of reverse offset printing: (a) initial, (b) coating (c) pattern generation (off step) and (d) transfer (set step). (e) Pattern examples of (top) a L/S 1 μm silver pattern and (bottom) a TFT array.

3. Ink formulation strategy and printed oxide TFTs

In the formulation of inks being compatible with ROP, a mixture of solvents is often adopted to control drying kinetics. We recently developed metal acetylacetonate inks with the ternary mixture system of toluene, methanol and iso-pentanol for ROP. Since toluene and methanol rapidly evaporate, a desired semidried state of the ink may be optimized by tuning the molar ratio of $MoO_2(acac)_2$ and iso-pentanol. A range of appropriate ratio for the transfer was found 50-60% and with such a composition, space resolution down to 200 nm was achieved. We have also demonstrated the solution-processed oxide TFTs showing the mobility of 0.17 $cm^2 V^{-1} s^{-1}$ with the SD electrode of printed conductive molybdenum oxide, which was formed by reducing $MoO_2(acac)_2$ ink by hydrogen plasma [1]. Recently, it was also proved that the indium nitrate dissolved in 2-methoxyethanol could be patterned by ROP and resulted printed In_2O_3 TFT performing at 1.4 $cm^2 V^{-1} s^{-1}$ was achieved with printed silver SD electrodes [2].

4. Patterning mechanism

The patterning phenomena in the ROP process was simulated using discrete element method (DEM). Here, a semidried ink layer was assumed as a bed of nanoparticles with JKR interactions and ignored forced strains originated from the deformation of PDMS to simplify the situation. Fig. 2a shows the snapshot of a transfer of a nanoparticle layer of thickness $h = 100$ nm removed by a plate surface with the size of $l_0 = 1$ μm moving at $V_z = 0.01$ m/s. Also, its time-lapsed cross-sections revealed that the particles beneath the cliché

surface first detached and then particles at the peripheral region gradually broke to complete the patterning process. Further, the cohesive energy densities between the constitutive nanoparticles $\sigma_{c,p}$ and between the particles and the bottom plate representing PDMS $\sigma_{a,p}$ were swept so as to investigate the effect of the particle interaction on the quality of particle transfers. Here, the following indicators $\chi_{rem} = 1 - N_{1,after}/N_{1,before}$ and $\chi_{ex} = N_{2,after}/N_{2,before}$ were used for the quality visualization in Fig. 2c-d where $N_{1,before}$ and $N_{1,after}$ are the number of particles at the initial and final conditions beneath the cliché, respectively, and $N_{2,before}$ and $N_{2,after}$ are the number of particles 'not' beneath the cliché at the initial and final conditions, respectively.

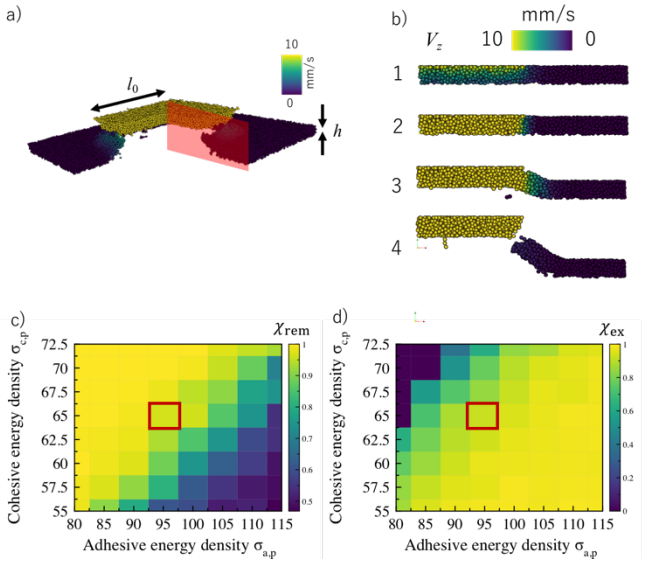

Fig.2 (a) A snapshot and (b) cross-sections of ROP patterning simulation by DEM. (c-d) Colormaps on patterning quality indicators χ_{rem} and χ_{ex} as functions of particle interactions $\sigma_{c,p}$ and $\sigma_{a,p}$. The condition shown in (a-b) is indicated by the red boxes.

Clearly, weaker adhesion of PDMS and higher particle cohesion were preferable for χ_{rem} to avoid the cohesive failure while reversed situations resulted in sharp edges (small χ_{ex}) because of easier fracturing of the layers. Well-balanced sets of $\sigma_{c,p}$ and $\sigma_{a,p}$ (red boxes in Fig. 3c-d, for example) satisfied a good patterning condition as both χ_{rem} and χ_{ex} were close to unity.

5. Processing rules in ROP

Processing parameters such as printing speed [3], printing pressure[4], overlay control [5] and PDMS configurations [6] are of particular importance in the practical application of ROP. In the presentation, the PDMS deformation will be highlighted as it plays a key role in many aspects of ROP process; for example, initial contact dynamics affects pattern quality in high-speed conditions, ink-filling into contact holes for vertically-interconnected devices and pattern size fidelity owning to local slipping of deformed PDMS (Fig. 3).

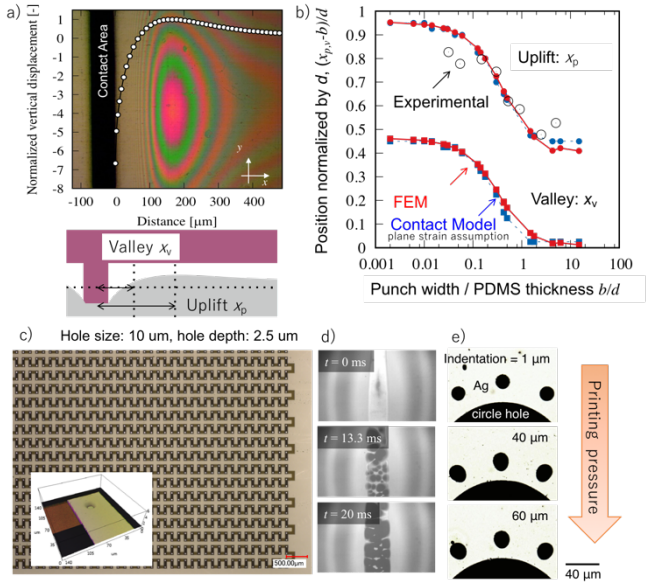

Fig.3 (a) Direct observation of PDMS deformation upon contact with a flat bar punch together with a predicted deformation profile. (b) PDMS pile-up phenomena. (c) Vertical interconnection enabled by the deformation of PDMS. (d) initial contact dynamics of PDMS blanket on a glass substrate. (e) pattern fidelity worsening phenomena originated from horizontal PDMS deformation.

3. Conclusions

In this paper, materials and processing rules of high-resolution printing (reverse offset printing) method was reviewed. The printed electronics should be tackled in concert from a multidisciplinary perspective as it involves various phenomena including nano-fracture mechanics, contact dynamics of soft materials such as adhesion and friction, chemical engineering processes such as drying, as well as ink formulations and device applications.

Acknowledgements

We would like to express sincere thanks to the JSPS KAKENHI Grant-in-Aid for Scientific Research C 19K05134 and the Japan Prize Foundation.

References

[1] Y. Kusaka, N. Shirakawa, S. Ogura, J. Leppäniemi, A. Sneck, A. Alastalo, H. Ushijima, N. Fukuda, ACS Appl. Mater. Interfaces 10 (2018) 24339–24343.

[2] J. Leppäniemi, A. Sneck, Y. Kusaka, N. Fukuda, A. Alastalo, Advanced Electronic Materials 15 (2019) 1900272–7.

[3] Y. Kusaka, M. Mizukami, T. Yamaguchi, N. Fukuda, H. Ushijima, J. Micromech. Microeng. 29 (2019) 045001–8.

[4] Y. Kusaka, S. Kanazawa, M. Koutake, H. Ushijima, J. Micromech. Microeng. 27 (2017) 105018.

[5] Y. Kusaka, K. Sugihara, M. Koutake, H. Ushijima, J. Micromech. Microeng. 24 (2014) 035020.

[6] Y. Kusaka, S. Kanazawa, N. Yamamoto, H. Ushijima, J. Micromech. Microeng. 27 (2017) 015003.